ARTICLES SCIENCE CHINA Materials

mater.scichina.com link.springer.com

https://doi.org/10.1007/s40843-019-9421-y

Sci China Mater 2019, 62(9): 1332–1340

Super-tough and strong nanocomposite fibers by flow-induced alignment of carbon nanotubes on grooved hydrogel surfaces

Chuangqi Zhao[1†], Pengchao Zhang[1,4†], Ruirui Shi[1], Yichao Xu[1], Longhao Zhang[1], Ruochen Fang[1], Tianyi Zhao[1*], Shuanhu Qi[1], Lei Jiang[1] and Mingjie Liu[1,2,3*]

ABSTRACT Nanocomposite fibers have attracted intensive attentions owing to their promising applications in various fields. However, the fabrication of nanocomposite fibers with super toughness and strong strength under mild conditions remains a great challenge. Here we present a facile flow-induced assembly strategy for the development of super-tough and strong nanocomposite fibers with highly ordered carbon nanotubes (CNTs), which can be induced by directional and fast flow on a grooved hydrogel surface. The prepared nanocomposite fibers show excellent mechanical properties, with a tensile strength up to 643±27 MPa and toughness as high as 77.3±3.4 MJ m^{-3} at ultimate strain of 14.8±1.5%. This versatile and efficient flow-induced alignment strategy represents a promising direction for the development of high-performance nanocomposites for practical applications.

Keywords: CNTs nanocomposite fibers, hydrogel surfaces, flow-induced assembly, super-toughness

INTRODUCTION

Biological materials, such as cartilages, skeletal muscles and nacres, are well known for their excellent strength and toughness due to the elaborate ordered microstructures of reinforcing nanomaterials within matrix [1–6]. Inspired by these sophisticated designs, tremendous efforts have been devoted to the development of bioinspired composites featuring strength and toughness competitive with that of their natural counterparts [7–10]. Advanced nanocomposites have been intensively developed by using carbon nanotubes (CNTs), graphene-oxide, and graphene owing to their superior mechanical properties. Nanocomposite fibers are of significance in constructing high-strength and high-toughness structural materials with low-weight in defense and aerospace engineering [11].

To date, several strategies have been developed to fabricate nanocomposite fibers with aligned structures, including spinning, microfluidic and confined space assisted assembly. The spinning-based method in wet [12–14] and dry state [15–17] has been widely utilized and has realized the fabrication of CNTs-based fibers or yarns with excellent tensile strength or toughness. However, the limitations of this method include that the fabrication process usually needs high concentration suspensions of CNTs or high energy consumption (i.e., high temperature) during the post-treatment process. Recently, two-dimensional (2D) nanomaterials, such as graphene-oxide or graphene, were introduced into the spinning system [18–20] in order to obtain better mechanical properties. However, the extremely rigorous post-treatment processes, such as UV irradiation, high-temperature annealing, and HI reduction, result in high cost, high energy consumption and high-risk of environmental pollution. The microfluidic-based strategy relies on complicated devices, making it difficult to scale up [21–24]. Although the confined space assisted assembly was developed to fabricate flexible and multi-functional graphene-based fiber with improved strength,

---

[1] Key Laboratory of Bio-Inspired Smart Interfacial Science and Technology of Ministry of Education, School of Chemistry, Beihang University, Beijing 100191, China

[2] International Research Institute for Multidisciplinary Science, Beihang University, Beijing 100191, China

[3] Beijing Advanced Innovation Center for Biomedical Engineering, Beihang University, Beijing 100191, China

[4] Present address: Department of Nanomedicine, Houston Methodist Research Institute, Houston, TX 77030, USA

[†] These authors contributed equally to this work.

[*] Corresponding authors (emails: liumj@buaa.edu.cn (Liu M); zhaoty@buaa.edu.cn (Zhao T))

magnetic and electrical properties [24–26], all the resulting nanocomposite fibers from the above strategies exhibit poor toughness, which is of great importance in military armor and aerospace [12]. Therefore, it is still a key hurdle to fabricate nanocomposite fibers with super toughness and strong strength under mild conditions.

Here, we developed a facile flow-induced assembly strategy for the development of super-tough and strong nanocomposite fibers with highly ordered CNTs. By using the liquid-like property of hydrogel surfaces and gravity, aqueous solutions containing CNTs could rapidly and directionally flow on the vertical hydrogel surfaces with grooves, leading to the assembly of CNTs into highly ordered structures. The assembled CNTs were converted into nanocomposite fibers, which exhibited the strength and toughness as high as 643±27 MPa and 77.3±3.4 MJ m^{-3}, respectively, at ultimate strain of 14.8±1.5%. Our nanocomposite fibers show significant energy absorption capacity at lower strain, which will have promising applications in advanced bullet-proof vest and protective layers.

EXPERIMENTAL SECTION

Materials

Acrylamide (AAm), sodium alginate (SA), ammonium persulphate (APS), calcium chloride ($CaCl_2$), *N*,*N*,*N′*,*N′*-tetramethylethylenediamine (TEMED), and *N*,*N′*-methylenebis(acrylamide) (MBAAm) were purchased from Sigma-Aldrich. High purified single-walled CNTs (average length: 5–30 μm (Fig. S1), purity: > 95%) dispersion (0.1 wt%) were purchased from the Nanjing XianFeng Nano Material Technology Co., Ltd. All the reagents were used without further purification.

Preparation of PAAm hydrogel

To obtain grooved polyacrylamide (PAAm) hydrogels, a copper wire with diameter of 0.5, 0.8, 1.0 or 1.2 mm was placed in the container as a template. The aqueous mixture of AAm (15 g), MBAAm (0.3 g), and APS (0.3 g) in 100 mL distilled water was prepared. The PAAm hydrogel was synthesized by radical polymerization for 5 min after the addition of TEMED (300 μL) at room temperature. Then the copper wire was peeled off and the obtained hydrogels were rinsed in excessive water to wash off the unreacted components, ensuring the grooved hydrogels fully swollen.

Preparation of reaction solution

SA powders were dissolved in deionized water and stirred overnight to obtain the alginate solution (2 wt%). The CNTs dispersion (0.1 wt%) was used as received. Then, the above stock solutions were added to deionized water to prepare various reaction solutions with different contents of SA and CNTs. The mixed solutions were sonicated for 10 min with 100 W power to obtain homogenous reaction solutions.

Preparation of bioinspired CNTs/CA nanocomposite fibers

Before the fabrication process, the prepared fully swollen grooved hydrogels were placed into equal weight of deionized water, then calcium chloride ($CaCl_2$) was added into the mixture and the final concentration was 0.05 mol $L^{-1.}$ After soaking for 30 min, the hydrogels containing $CaCl_2$ were obtained. To fabricate CNTs/calcium alginate (CA) nanocomposite fibers, the prepared reaction solution was dropped onto the grooved hydrogel surface. Upon contacting the hydrogel surface, the droplet of the reaction solution rapidly flowed along the groove on the hydrogel surfaces due to the liquid-like property of hydrogel surfaces and gravity. At the same time, the reaction solution was gelatinized into a gel fiber rapidly *via in situ* ionically crosslinking of CA as the calcium ions diffused from the hydrogel surface to the liquid film. The gel fibers were readily separated from the hydrogel surface in water bath. After being dried in air condition, uniform and continuous nanocomposite fibers were obtained.

Instruments and characterization

The viscosity of the reaction solutions was measured at 21°C by using an Anton Paar model MCR-301 rheometer in a range of 1–100 rad s^{-1}. The morphology of the obtained fibers was characterized by scanning electron microscopy (SEM, JEOL SU8010, Japan) operated at 5 kV. To minimize charging effects, a few nanometers thick layer of platinum was applied to nonconductive samples prior to imaging. Polarized optical microscopy was performed under crossed polarizers by using a Nikon model Eclipse LV100NPOL polarized optical microscope (POM).

Mechanical testing of nanocomposite fibers

Stress-strain curves were obtained by testing the samples using a mechanical strength tester ESM301 from Mark-10 Corporation. Tests were performed at a rate of 0.5 mm min^{-1}. The mechanical properties for each sample were based on the average value of three specimens. The prepared fibers were equilibrated under 25°C and 10% relative humidity condition for 48 h before the mechanical testing, and the cross-section areas of all samples were calculated by SEM. The Young's modulus of the samples was determined by the slope of the linear region of the stress-strain curves.

RESULTS AND DISCUSSION

It is well known that flow can facilitate the assembly of nanomaterials [27–29]. Several studies have demonstrated the preparation of nanocomposite fibers with aligned 2D nanosheets or 1D nanotubes by using wet-spinning strategy. However, concentrated suspensions of nanomaterials and the relatively low flow rates pose difficulties in achieving high-level alignment of nanomaterials [27]. Recently, we observed that liquid droplets can rapidly spread on an immiscible oil/hydrogel interface in a liquid/liquid/gel system [30–32]. In this work, we used the CNTs that were well dispersed in aqueous solution with a surfactant that adsorbs at the surface of the nanotube bundles. These suspensions did not coarsen or phase-separate macroscopically over several weeks. SA is soluble in water and forms stable gels at room temperature in the presence of divalent cations (i.e., Ca^{2+}, calcium ions). Ca^{2+} ions crosslinked alginates have been widely used in biomedical applications [33]. Here, we demonstrate that a droplet of low-viscosity reaction solution containing CNTs and alginate could rapidly and directionally flow on the vertical hydrogel grooves, facilitating the alignment of CNTs along the flow direction.

Fig. 1 illustrates the fabrication process of bioinspired CNTs/CA nanocomposite fibers. The reaction solution containing CNTs was dropped from the top of the vertical hydrogel surface with a uniform groove (Fig. 1a). Owing to the liquid-like property of the hydrogel surfaces and gravity, the reaction solution could rapidly and directionally flow along the groove. The CNTs are expected to form a preferential orientation in the flow direction induced by the shear-flow. This transiently ordered structure can preserve *via in situ* ionic crosslinking of alginate by Ca^{2+} ions that diffused from the hydrogel surfaces, converting the CNTs-containing solution layer into a CA gel fiber. This CA gel fiber can be readily separated from the grooves after immersion in a water bath (Fig. S2). After being dried in air, the gel fiber shrank significantly, keeping the same length while reducing eight times in diameter compared with the wet one. Importantly, the assembled CNTs still maintained during the drying process (Fig. S3). Meanwhile, the drastic contraction in the diameter direction and the capillary force during the loss of water could help close packing the CNTs within the CA matrices. Consequently, the CNTs become densely stacked and relatively aligned directionally to the fiber's axis. The dried CNTs/CA nanocomposite fibers were flexible and strong enough so that they could be wound around a spool (Fig. 1b) or knot without the occurrence of any breakage (Fig. S4), demonstrating their excellent flexibility and resistance to torsion. The uniform morphology of the CNTs/CA nanocomposite fibers shown in Fig. 2c suggests that the CNTs are assembled into uniform and continuous nanocomposite fibers without defects. The cross-section morphology of the nanocomposite CNTs/CA fibers shows a typical close-packed microstructure of CNTs (Fig. 2d). The energy dispersive X-ray spectroscopy (EDS) result indicates the uniform distribution of Ca element, revealing that the Ca^{2+} ions are fully diffused and uniformity distributed in the CNTs/CA nanocomposite fibers (Fig. S5).

Both the fast flow and the confined grooves are highly desirable to achieve high-level orientation of CNTs [34]. We investigated the influence of flow rate on the degree of orientation of CNTs by placing the hydrogel grooves horizontally (0°), 45° tilt and vertically (90°). The prepared nanocomposite fibers were characterized by using wide-angle X-ray scattering (WAXS) and POM (Fig. 2). With increasing inclination angle of the hydrogel grooves from 0° to 90°, the flow rates increased from ca. 1 mm s^{-1} to ca. 3 mm s^{-1} (Fig. S6), facilitating the orientated assembly of CNTs. The 2D WAXS pattern of the CNTs/CA nanocomposite fibers prepared on the vertical hydrogel grooves shows strong diffuse spots, indicating the high alignment of CNTs in the nanocomposite fibers. In contrast, the CNTs/CA nanocomposite fiber prepared on the horizontal hydrogel grooves shows an isotropic scattering pattern, indicating the random distribution of CNTs within the fiber. The results of POM characterization are consistent with the 2D WAXS results. The POM image of the CNTs/CA nanocomposite fibers prepared on the vertical hydrogel grooves under crossed polarizers shows a contrast at every 45° on rotation, giving a completely dark image when the azimuthal angle between the polarized direction of the incident light and the axis of fiber was either 0° or 90° (Fig. S7). These results suggest that the CNTs aligned during the directional and fast flow were preserved and predominantly oriented along the axis of the fibers.

The orientation of CNTs significantly affects the mechanical performance of the resulting nanocomposite fibers. We first compared the typical stress-strain curves of the CNTs/CA nanocomposite fibers prepared on hydrogel grooves with different angles of inclination (i.e., 0°,

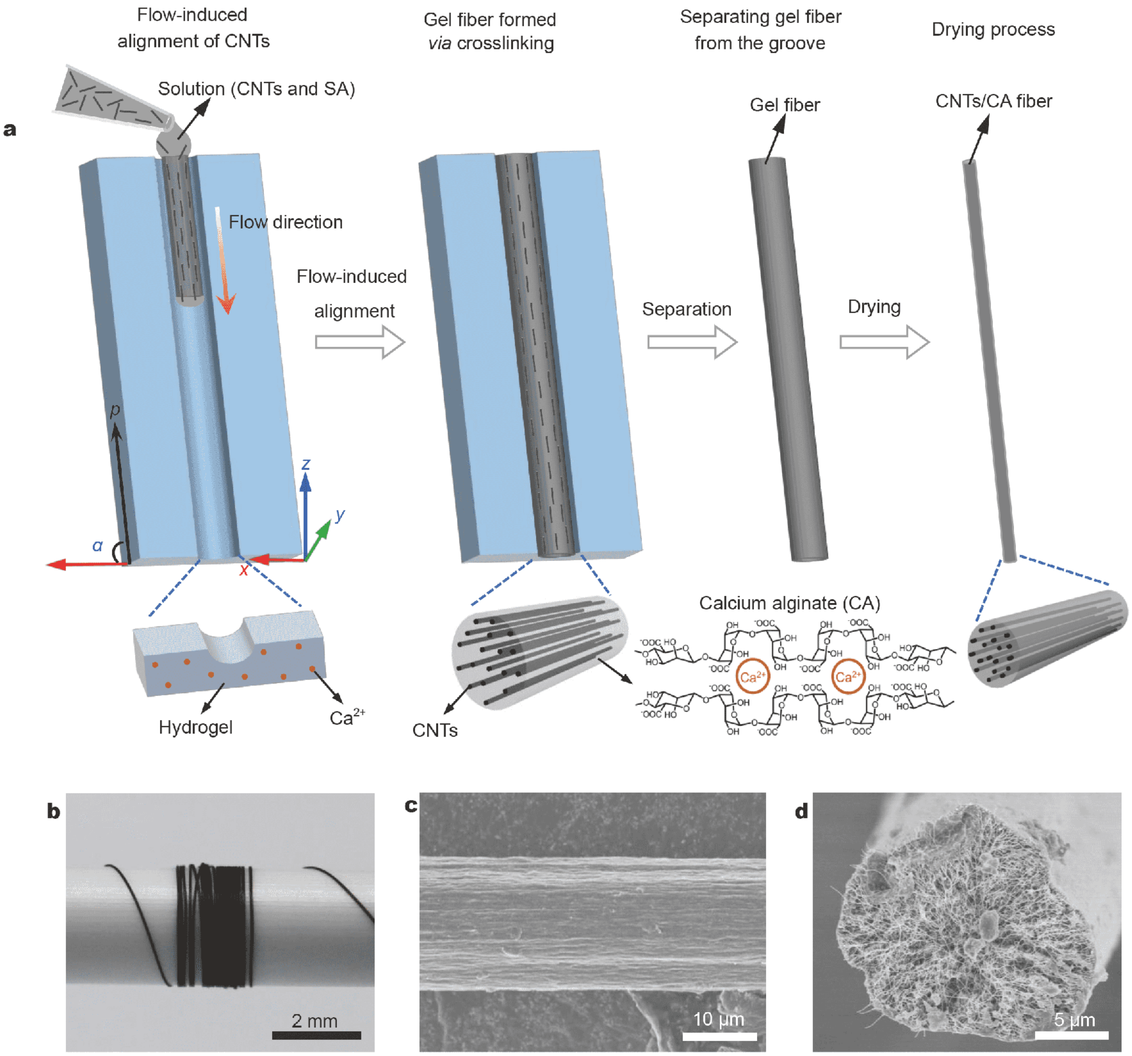

Figure 1 Schematic illustration of the preparation of bioinspired CNTs/CA nanocomposite fibers. (a) Along with the solutions containing CNTs and SA flowing through the groove on the hydrogel surface, the shear-flow induced the alignment of CNTs. Then the aligned CNTs were fixed by *in situ* cross-linking of alginate with Ca^{2+} ions, which diffused from the hydrogel surface to the solution layer. The formed gel fibers can be readily separated from the hydrogel groove after immersion in a water bath. After thorough and repeated washing with water and subsequent drying in ambient conditions, uniform and continuous CNTs/CA nanocomposite fiber without defects was obtained. (b) Digital photograph of the CNTs/CA nanocomposite fiber collected on a circular tube. (c, d) SEM images of (c) surface and (d) cross-section morphology of the CNTs/CA nanocomposite fiber.

45°, and 90°) (Fig. 3a). Among them, the nanocomposite fibers prepared on the vertical hydrogel grooves, which have highly aligned CNTs, show the best mechanical performance, with the tensile strength and toughness of as high as 643±27 MPa and 77.3±3.4 MJ m^{-3}, respectively (Fig. 3b). In contrast, the nanocomposite fibers prepared on the horizontal hydrogel grooves, which show randomly distributed CNTs, exhibit the lowest tensile strength and toughness. These results indicate that our flow-induced assembly strategy can effectively facilitate the alignment of CNTs into highly ordered structures, leading to the superior mechanical properties.

To verify the essential role of confined grooves in the realization of highly aligned CNTs, the hydrogel grooves with four different width (0.5, 0.8, 1.0 and 1.2 mm) were employed to fabricate nanocomposite fibers on vertically placed grooved hydrogel surfaces. In such case, the prepared nanocomposite fibers show increased diameters from ca. 15 μm to ca. 32 μm as the width of the hydrogel grooves increases (Figs S8, S9). As shown in Fig. 3c, both the tensile strength and toughness decrease as the increase of groove width from 0.5 to 1.2 mm. We supposed that the smaller sized of the groove width, the more restricted Brownian diffusion of CNTs, and the more

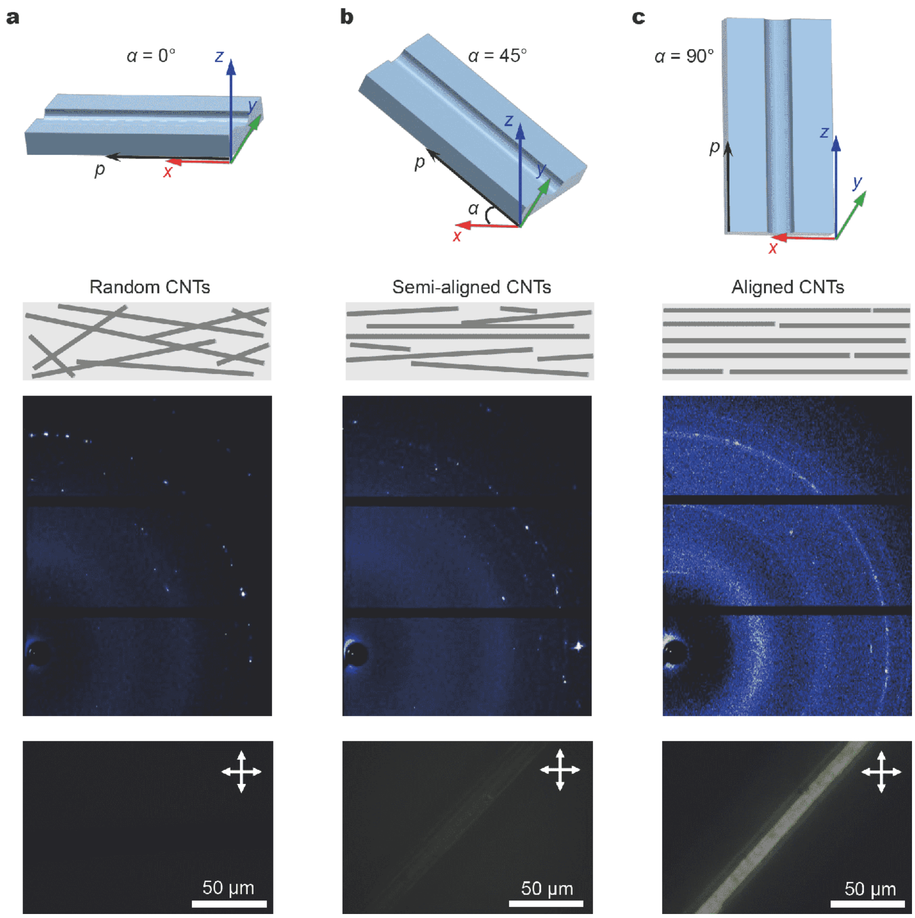

Figure 2 Structural characterization of the prepared bioinspired CNTs/CA nanocomposite fibers. Schematic (top), 2D WAXS images (middle) and POM images (bottom) of the CNTs/CA nanocomposite fibers prepared at (a) 0°, (b) 45° and (c) 90° inclination of the hydrogel grooves.

favorable to align CNTs in the flow direction, thus better mechanical properties of the prepared fibers [24]. These results suggest that the confined grooves also play an essential role in achieving the alignment of CNTs, which is the key to realize the exceptional improvement of the mechanical performance.

Importantly, the ratio of the CNTs to SA is easily adjusted, which makes our methods distinctively easier than the current assembly strategies. We investigated the influence of the ratios of CNTs to SA (0.2, 0.6, 1.0, 1.4, and 1.8 wt%) on the mechanical performance of the CNTs/CA nanocomposite fibers. The viscosities of all these reaction solutions were lower than 9 mPa s (Fig. S10) and the solutions could flow through the hydrogel grooves quickly. The mechanical properties of the CNTs/CA composite fibers with different CNTs contents are compared in Fig. 3d and listed in detail in Table S1. The CNTs/CA composite fibers with about 0.6 wt% of CNTs to SA reach the maximum value of tensile strength and toughness. For other conditions, the tensile strength and toughness of the CNTs/CA composite fibers decreased. When the concentration of CNTs in the reaction solutions was lower than 0.2 wt%, the lack of filler crippled the load carrying capacity of the nanocomposite fibers (Figs S11, S12). On the contrary, too high concentration of CNTs in the reaction solutions may destroy the highly ordered structures of CNTs (Figs S13–S15), thus decreasing the tensile strength and toughness of the nanocomposite fibers [35–37].

Our CNTs/CA nanocomposite fibers display excellent tensile strength and a record high toughness of 77.3± 3.4 MJ m^{-3}, which is four times higher than that of the reported graphene-based fibers (Fig. 4a and Tables S2–S4). The super-high toughness of our CNTs/CA composite fibers derives from the combination of high elongation-to-break and relatively high-yield strength (Fig. 4b). The reported graphene-based fibers assembled by the wet-spinning process exhibited a tensile strength of

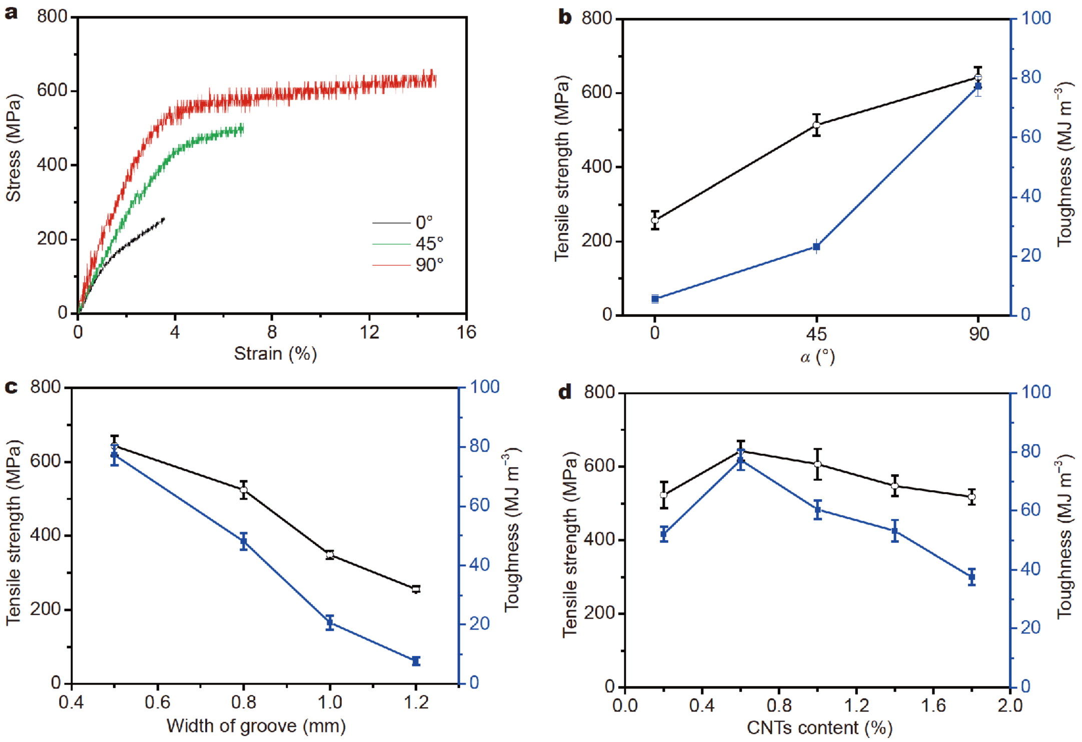

Figure 3 Mechanical performance of the bioinspired CNTs/CA nanocomposite fibers. (a) Typical stress-strain curves and (b) strength and toughness of the CNTs/CA composite fibers prepared at different inclination angles of the hydrogel grooves. (c, d) The strength and toughness of CNTs/CA composite fibers prepared by (c) hydrogel grooves with different widths and (d) different CNTs contents.

740.1 MPa [38], slightly higher than our nanocomposite fibers. However, the toughness of these graphene-based fibers is only 18.7 MJ m^{-3}, far lower than our CNTs/CA composite fibers. On the contrary, the CNTs reinforced rGO-SWNT-PVA fibers in previous work [20] show less than 20 MJ m^{-3} at strain about 20%, although their toughness could reach 1,388 MJ m^{-3} with high strain of about 350%. Therefore, our bioinspired CNTs/CA nanocomposite fibers have much higher energy absorption capacity at lower strain (less than 20%) [12]. Moreover, the tensile strength of this rGO-SWNT-PVA fibers is only 570 MPa, lower than that of our CNTs/CA nanocomposite fibers (643 MPa).

To further explore the toughness mechanism of the CNTs/CA nanocomposite fibers, the fracture morphologies of the fibers after tensile tests are shown in Fig. 4c, d. It can be clearly seen that the aligned CNTs in the axis direction are pulled out, demonstrating the relatively slippage occurs between the CNTs and the CA matrices, which can toughen the fibers by increasing the strain to failure at high tensile strength and result in the super fracture toughness.

The proposed fracture mode of CNTs/CA composite fibers is illustrated to understand the mechanism of synergistic high tensile strength and toughness, as shown in Fig. 4e. In the initial stage, the aligned CNTs along with the ionic bonding CA around them bear the tensile stress. No matrices cracks or relatively slippage occurred and less energy was absorbed by the fibers in this elastic deformation stage. With gradually increasing loading, the CA matrices are further stretched and some microcrack appears. The fiber can absorb more energy in this plastic deformation stage. As further increasing the load, viscous sliding between CNTs and the CA matrices occurs, which results in significant strain and energy dissipation [39,40].

CONCLUSIONS

In conclusion, we have developed a facile and effective flow-induced assembly strategy to synthesize bioinspired CNTs/CA nanocomposite fibers with high alignment of CNTs. The tensile strength and toughness of these CNTs/CA nanocomposite fibers reach up to 643±27 MPa and 77.3 MJ m^{-3}, respectively, exhibiting significant energy absorption capacity at a low strain of about 14.8%. In addition, the composition of the CNTs/CA nanocompo-

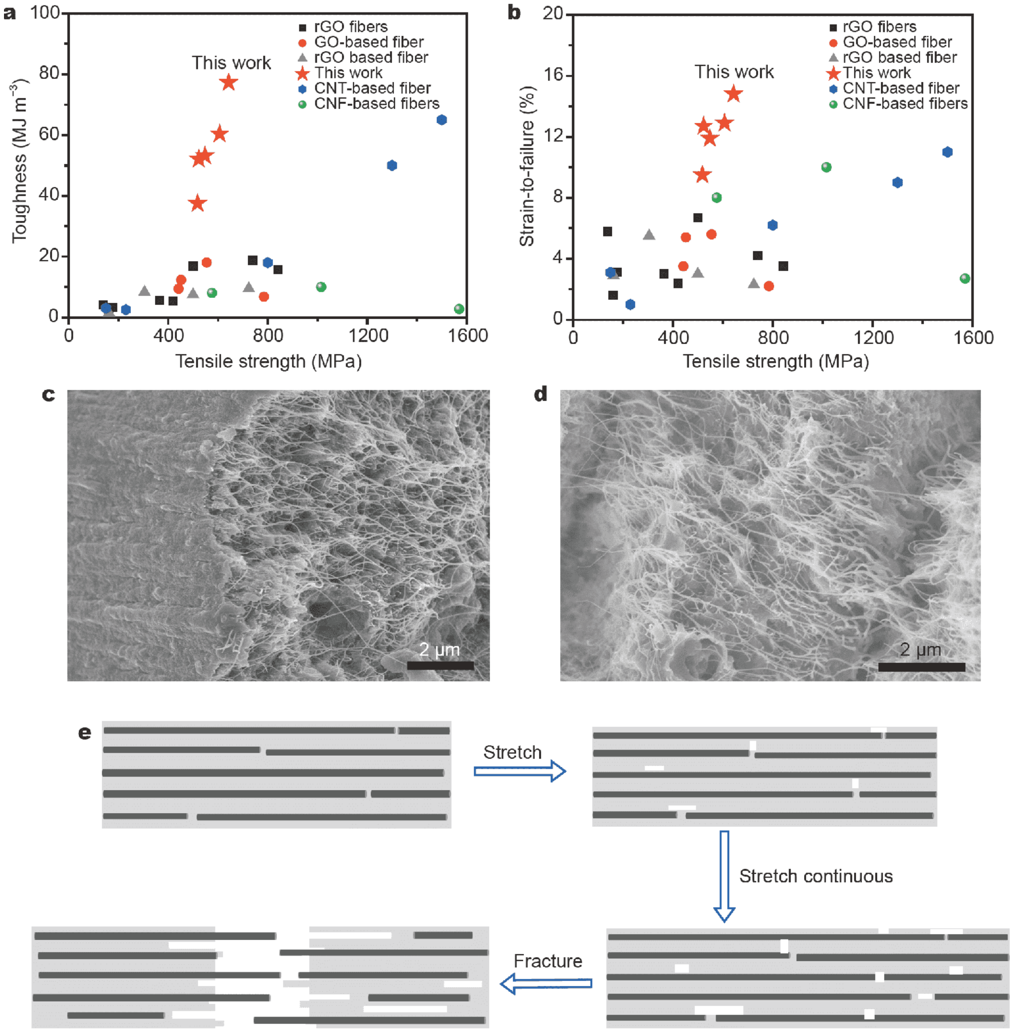

Figure 4 The comparison of (a) toughness and (b) strain-to-failure of the CNTs/CA nanocomposite fibers with other graphene or GO-based nanocomposite fibers. The toughness and strain-to-failure of our CNTs/CA nanocomposite fibers are higher than that of all reported graphene-based fibers to date. (c) Inclined-view and (d) side-view SEM images of the fracture morphologies of the bioinspired CNTs/CA nanocomposite fibers. (e) Schematic diagram illustrating the proposed fracture mechanism of the CNTs/CA nanocomposite fibers.

site fibers can be easily adjusted, leading to a high tunability in flexibility and property. This novel assembly strategy and the outstanding mechanical properties of the CNTs/CA nanocomposite fibers would be of great interest to researchers who work in multiple disciplines, including carbon-based nanomaterials, structural composites, engineering and technology-related fields etc., and could inspire further explorations to high-performance composites.

Received 21 February 2019; accepted 23 March 2019;

1 Addadi L, Weiner S. A pavement of pearl. Nature, 1997, 389: 912–913
2 Mayer G. Rigid biological systems as models for synthetic composites. Science, 2005, 310: 1144–1147
3 Kim HN, Jiao A, Hwang NS, *et al.* Nanotopography-guided tissue engineering and regenerative medicine. Adv Drug Deliver Rev, 2013, 65: 536–558
4 Keene DR. Ultrastructure of type VI collagen in human skin and cartilage suggests an anchoring function for this filamentous network. J Cell Biol, 1988, 107: 1995–2006
5 Zhao Z, Fang R, Rong Q, *et al.* Bioinspired nanocomposite hydrogels with highly ordered structures. Adv Mater, 2017, 29: 1703045
6 Wegst UGK, Bai H, Saiz E, *et al.* Bioinspired structural materials. Nat Mater, 2015, 14: 23–36
7 Gao HL, Chen SM, Mao LB, *et al.* Mass production of bulk artificial nacre with excellent mechanical properties. Nat Commun,

2017, 8: 287
8 Mao LB, Gao HL, Yao HB, *et al.* Synthetic nacre by predesigned matrix-directed mineralization. Science, 2016, 354: 107–110
9 Cui Y, Gong H, Wang Y, *et al.* A thermally insulating textile inspired by polar bear hair. Adv Mater, 2018, 30: 1706807
10 Du G, Mao A, Yu J, *et al.* Nacre-mimetic composite with intrinsic self-healing and shape-programming capability. Nat Commun, 2019, 10: 800
11 Lu W, Zu M, Byun JH, *et al.* State of the art of carbon nanotube fibers: opportunities and challenges. Adv Mater, 2012, 24: 1805–1833
12 Miaudet P, Badaire S, Maugey M, *et al.* Hot-drawing of single and multiwall carbon nanotube fibers for high toughness and alignment. Nano Lett, 2005, 5: 2212–2215
13 Dalton AB, Collins S, Muñoz E, *et al.* Super-tough carbon-nanotube fibres. Nature, 2003, 423: 703
14 Vigolo B. Macroscopic fibers and ribbons of oriented carbon nanotubes. Science, 2000, 290: 1331–1334
15 Jiang K, Li Q, Fan S. Spinning continuous carbon nanotube yarns. Nature, 2002, 419: 801
16 Zhang M, Atkinson KR, Baughman RH. Multifunctional carbon nanotube yarns by downsizing an ancient technology. Science, 2004, 306: 1358–1361
17 Li YL, Kinloch IA, Windle AH. Direct spinning of carbon nanotube fibers from chemical vapor deposition synthesis. Science, 2004, 304: 276–278
18 Lu Z, Foroughi J, Wang C, *et al.* Superelastic hybrid CNT/graphene fibers for wearable energy storage. Adv Energy Mater, 2017, 8: 1702047
19 Wang R, Sun J, Gao L, *et al.* Fibrous nanocomposites of carbon nanotubes and graphene-oxide with synergetic mechanical and actuative performance. Chem Commun, 2011, 47: 8650–8652
20 Shin MK, Lee B, Kim SH, *et al.* Synergistic toughening of composite fibres by self-alignment of reduced graphene oxide and carbon nanotubes. Nat Commun, 2012, 3: 650
21 Xin G, Zhu W, Deng Y, *et al.* Microfluidics-enabled orientation and microstructure control of macroscopic graphene fibres. Nat Nanotech, 2019, 14: 168–175
22 Mittal N, Ansari F, Gowda.V K, *et al.* Multiscale control of nanocellulose assembly: transferring remarkable nanoscale fibril mechanics to macroscale fibers. ACS Nano, 2018, 12: 6378–6388
23 Mittal N, Jansson R, Widhe M, *et al.* Ultrastrong and bioactive nanostructured bio-based composites. ACS Nano, 2017, 11: 5148–5159
24 Håkansson KMO, Fall AB, Lundell F, *et al.* Hydrodynamic alignment and assembly of nanofibrils resulting in strong cellulose filaments. Nat Commun, 2014, 5: 4018
25 Ma T, Gao HL, Cong HP, *et al.* A bioinspired interface design for improving the strength and electrical conductivity of graphene-based fibers. Adv Mater, 2018, 30: 1706435
26 Dong Z, Jiang C, Cheng H, *et al.* Facile fabrication of light, flexible and multifunctional graphene fibers. Adv Mater, 2012, 24: 1856–1861
27 Papthanasiou TD, Guell DC. Flow-Induced Alignment in Composite Materials. Cambridge: Woodhead Publishing Ltd., 1997
28 Kataoka DE, Troian SM. Patterning liquid flow on the microscopic scale. Nature, 1999, 402: 794–797
29 Su B, Lu X, Lu Q. A facile method to prepare macroscopically oriented mesostructured silica film: controlling the orientation of mesochannels in multilayer films by air flow. J Am Chem Soc, 2008, 130: 14356–14357
30 Zhang P, Zhang F, Zhao C, *et al.* Superspreading on immersed gel surfaces for the confined synthesis of thin polymer films. Angew Chem Int Ed, 2016, 55: 3615–3619
31 Zhao C, Zhang P, Gu Z, *et al.* Superspreading-based fabrication of asymmetric porous PAA-g-PVDF membranes for efficient water flow gating. Adv Mater Interfaces, 2016, 3: 1600615
32 Hao Q, Zhao C, Sun B, *et al.* Confined synthesis of two-dimensional covalent organic framework thin films within superspreading water layer. J Am Chem Soc, 2018, 140: 12152–12158
33 Xie L, Jiang M, Dong X, *et al.* Controlled mechanical and swelling properties of poly(vinyl alcohol)/sodium alginate blend hydrogels prepared by freeze-thaw followed by Ca^{2+} crosslinking. J Appl Polym Sci, 2012, 124: 823–831
34 Gunes DZ, Scirocco R, Mewis J, *et al.* Flow-induced orientation of non-spherical particles: effect of aspect ratio and medium rheology. J Non-Newtonian Fluid Mech, 2008, 155: 39–50
35 Chen SM, Gao HL, Zhu YB, *et al.* Biomimetic twisted plywood structural materials. Natl Sci Rev, 2018, 5: 703–714
36 Wang JL, Hassan M, Liu JW, *et al.* Nanowire assemblies for flexible electronic devices: recent advances and perspectives. Adv Mater, 2018, 30: 1803430
37 Song P, Qin H, Gao HL, *et al.* Self-healing and superstretchable conductors from hierarchical nanowire assemblies. Nat Commun, 2018, 9: 2786
38 Zhang Y, Peng J, Li M, *et al.* Bioinspired supertough graphene fiber through sequential interfacial interactions. ACS Nano, 2018, 12: 8901–8908
39 Pan XF, Gao HL, Lu Y, *et al.* Transforming ground mica into high-performance biomimetic polymeric mica film. Nat Commun, 2018, 9: 2974
40 Zhao N, Yang M, Zhao Q, *et al.* Superstretchable nacre-mimetic graphene/poly(vinyl alcohol) composite film based on interfacial architectural engineering. ACS Nano, 2017, 11: 4777–4784

Acknowledgements This research was supported by the National Key R&D Program of China (2017YFA0207800), the National Natural Science Foundation of China (21574004), the National Natural Science Funds for Distinguished Young Scholar (21725401), the 111 project (B14009), the Fundamental Research Funds for the Central Universities, the National "Young Thousand Talents Program", and the China Postdoctoral Science Foundation (2017M620012).

Author contributions Zhao C, Zhang P and Liu M designed the project. Zhao C, Shi R preformed the experiments. Zhao C, Zhang P, Xu Y, Zhang L, Fang R, Zhao T and Qi S analyzed the results. Zhao C, Zhang P, Zhao T and Liu M wrote the paper. All authors contributed to general discussion of the article.

Conflict of interest The authors declare that they have no conflict of interest.

Supplementary information Supplementary materials are available in the online version of the paper.

Chuangqi Zhao is currently a PhD student at Beihang University. He received his BSc degree in materials science from Changchun University of Technology (China) in 2012, MSc degree in applied chemistry from Beihang University (China) in 2015. Then, he joined Prof. Lei Jiang's group at Beihang University. His current research interests focus on the superwettability and applications of bioinspired gel materials and development of novel bio-inspired multi-functional, high performance layered nanocomposite materials.

Pengchao Zhang received his BSc degree in materials science (2010) from Wuhan University of Technology (WHUT), China. Then, he joined Prof. Lei Jiang's group and received PhD degree from the Institute of Chemistry, Chinese Academy of Sciences (ICCAS) (2016). He currently holds a postdoctoral position in Houston Methodist Research Institute/Weill Cornell Medical College. His current research interests focus on the superwettability and applications of bioinspired gel materials and development of novel microfluidics for single cell analysis.

Tianyi Zhao is an associate professor at Beihang University. She received her BSc degree from Jilin University in 2004. Then, she joined Prof. Lei Jiang's group and received PhD degree from ICCAS in 2010. She then worked as an assistant professor in Beihang University. Her current research interests focus on bioinspired materials with super-wettability and their applications in catalytic fields.

Mingjie Liu is currently a full-time professor at Beihang University. In 2005, he joined Prof. Lei Jiang's group and received his PhD degree from the National Center for Nanoscience and Technology, Chinese Academy of Sciences (2010). He then worked as a postdoc in Prof. Takuzo Aida's group in Riken in Japan from 2010 to 2015. In 2015, he was awarded the "1000 Youth Plan program" and joined Beihang University. In 2017, he was awarded the National Science Fund for Distinguished Young Scholars. His current research interests focus on anisotropic soft matter with ordered structures, bioinspired design, and application of gel materials.

水凝胶表面沟槽内液流诱导制备具有取向碳纳米管的超韧高强纳米复合纤维

赵创奇[1†], 张鹏超[1,4†], 史蕊蕊[1], 许一超[1], 张龙昊[1], 房若辰[1],
赵天艺[1*], 齐栓虎[1], 江雷[1], 刘明杰[1,2,3*]

摘要 纳米复合纤维由于其广泛的应用前景受到科学家的关注. 但是在温和条件下制备具有优异断裂韧性与高强度的纳米复合纤维仍然面临很大的挑战. 本文中, 我们展示了一种简单的基于液流组装的策略用于制备具有超高断裂韧性与强度的纳米复合纤维. 在准液态的水凝胶表面和重力的双重作用下, 含有碳纳米管的水溶液可以沿水凝胶沟槽极快速地流动, 从而诱导碳纳米管取向排列. 我们制备出的纳米复合纤维拉伸强度和断裂韧性分别高达643±27 MPa和77.3±3.4 MJ m^{-3}, 极限断裂伸长率14.8±1.5%. 这种具有较强普适性和高效率的液流诱导取向策略为高性能纳米复合纤维的实际应用提供了新的可行的发展方向.